SFB/CPP-10-111
TTP10-47

Higgs boson production in gluon fusion to NNLO in the MSSM

Alexey Pak, Matthias Steinhauser, Nikolai Zerf

Institut für Theoretische Teilchenphysik
Karlsruhe Institute of Technology (KIT)
76128 Karlsruhe, Germany

Abstract

We consider the Higgs boson production in the gluon-fusion channel to next-to-next-to-leading order within the Minimal Supersymmetric Standard Model. In particular, we present analytical results for the matching coefficient of the effective theory and study its influence on the total production cross section in the limit where the masses of all MSSM particles coincide. For supersymmetric masses below 500 GeV we observe a significant enhancement of the Standard Model cross section, the K factor, however, changes only marginally.

PACS numbers: 12.38.Bx 14.80.Bn

1 Introduction

The hunt for the Higgs boson is performed with great enthusiasm both at the Fermilab Tevatron and at the CERN Large Hadron Collider (LHC). The Higgs boson constitutes the last missing piece in the Standard Model (SM) of particle physics and could explain the generation of mass terms in the Lagrange density. The latter is also true in many extensions of the SM, such as supersymmetry.

In the recent years many higher order corrections to production and decay of the Higgs boson have been computed. The most recent computations within the SM that appeared in the end of 2009 [1–3] describe the Higgs boson production in gluon fusion at the next-to-next-to-leading order (NNLO) taking the finite top quark mass into account. An important outcome of these papers is the justification to use the effective theory (built for the infinite top quark mass) for the evaluation of the cross section as it was done in Refs. [4–6]. It is suggestive that this conclusion also holds for the Minimal Supersymmetric Standard Model (MSSM) since the corresponding calculation would have a similar structure. At NLO this has been demonstrated in Refs. [7, 8]. In this paper we assume that it also holds at NNLO in situation when all supersymmetric particles are heavier than the top quark.

The supersymmetric NLO correction to the gluon fusion process has been considered in various papers. In Refs. [7, 9] the Higgs boson production cross section (and the decay rate) have been computed in the effective theory framework and thus applies to Higgs boson masses less than about 200 GeV. The results have been confirmed by a (numerical) calculation in the full theory [8] (see also Refs. [10, 11]). It should be mentioned that the squark contribution has been considered separately in Refs. [12, 13]. Furthermore, an estimate of the NNLO supersymmetric corrections was presented in Ref. [14] (see also Ref. [7]) assuming that the NNLO corrections to the matching coefficient in the MSSM and the SM are numerically of the same order.

In this paper we consider the strong interaction part of the MSSM and evaluate the total production cross section of an intermediate mass Higgs boson in the process of gluon fusion. As motivated above, we employ the effective theory obtained in the formal limit where all supersymmetric particles and the top quark are infinitely heavy, which leads to the Lagrange density

$$\mathcal{L}_{Y,\text{eff}} = -\frac{\phi^0}{v^0} C_1^0 \mathcal{O}_1^0 + \mathcal{L}_{QCD}^{(5)}\,, \tag{1}$$

with

$$\mathcal{O}_1^0 = \frac{1}{4} G_{\mu\nu}^0 G^{0,\mu\nu}\,. \tag{2}$$

C_1^0 is the coefficient function containing the remnant contributions of the heavy particles and $\mathcal{O}_1^0$ is the effective operator. $\mathcal{L}_{QCD}^{(5)}$ is the QCD Lagrange density with five active flavours. In our case ϕ^0 denotes the light CP-even Higgs boson of the MSSM. $G_{\mu\nu}^0$ is the

gluonic field strength tensor of the standard five-flavour QCD and the superscript "0" indicates bare quantities. Note that the renormalization of ϕ^0/v^0 is of higher order in the electromagnetic coupling constant.

The renormalization of $\mathcal{O}_1^0$ is discussed in detail in Refs. [15, 16]. For completeness we reproduce here the renormalization constant which in the $\overline{\rm MS}$ scheme is given by

$$\mathcal{O}_1 = Z_{11}\,\mathcal{O}_1^0\,, \qquad Z_{11} = \left(1 - \frac{\pi}{\alpha_s}\frac{\beta^{(5)}}{\epsilon}\right)^{-1}\,, \tag{3}$$

where $d = 4 - 2\epsilon$ is the space-time dimension and $\beta^{(5)} = \beta^{(5)}(\alpha_s)$ is the β function of the standard five-flavour QCD with $\beta^{(5)} = -(\alpha_s^{(5)}/\pi)^2\beta_0^{(5)} + \ldots$ and $\beta_0^{(n_l)} = 11/4 - n_l/6$. Since $C_1^0\mathcal{O}_1^0 = C_1\mathcal{O}_1$, the coefficient function is renormalized with $1/Z_{11}$.

Following Ref. [17], we slightly redefine the coefficient function and the operator in order to have objects which are separately renormalization group invariant. Introducing

$$\begin{aligned} \mathcal{O}_g &= B^{(5)}\mathcal{O}_1\,, \\ C_g &= \frac{1}{B^{(5)}}C_1\,, \end{aligned} \tag{4}$$

with

$$B^{(5)} = -\frac{\pi^2\beta^{(5)}}{\beta_0^{(5)}\alpha_s^{(5)}}\,, \tag{5}$$

we may choose independently the "soft" and the "hard" renormalization scales. Our following analysis of the Higgs production cross section takes advantage of those properties of $\mathcal{O}_g$ and C_g. Note that the LO piece of C_g is not proportional to α_s.

In this paper we consider the strongly interacting part of the MSSM and assume for simplicity the degenerate supersymmetric mass spectrum. The evaluation of the coefficient functions is performed within Dimensional Reduction (`DRED`) [18] where we follow Refs. [19, 20] for the practical implementation.

The remainder of the paper is organized as follows: in the following section we briefly revisit the SM and in particular discuss the effect of $B^{(5)}$ introduced above. We furthermore evaluate the SM coefficient function within `DRED` which is a useful preparation for the SUSY QCD calculation. Next, in Section 3 we discuss the three-loop calculation of the MSSM coefficient function which is used in Section 4 to compute the cross section to NNLO. Section 5 contains the summary and conclusions.

2 Revisiting the SM

As mentioned in the Introduction, the gluon fusion process has been discussed extensively in the literature. The purpose of this Section is twofold: on the one hand we want to

discuss the effect of $B^{(5)}$ introduced in Eq. (4) on the numerical predictions, on the other hand we repeat the SM calculation in the framework of DRED as a preparation for the calculation in the supersymmetric theory.

2.1 Separation of hard and soft scales

The SM coefficient function expressed in terms of the on-shell top quark mass and the five-flavour strong coupling reads[1] [16, 21] (see also Ref. [22]):

$$\begin{aligned} C_1^{\rm SM} &= -\frac{1}{3}\frac{\alpha_s^{(5)}}{\pi}\Bigg\{1+\frac{\alpha_s^{(5)}}{\pi}\frac{11}{4} \\ &\quad + \left(\frac{\alpha_s^{(5)}}{\pi}\right)^2\left[\frac{2777}{288}+\frac{19}{16}\ln\frac{\mu^2}{M_t^2}+n_l\left(-\frac{67}{96}+\frac{1}{3}\ln\frac{\mu^2}{M_t^2}\right)\right]\Bigg\}, \end{aligned} \tag{6}$$

where $n_l = 5$ is the number of massless quarks.

In Fig. 1(a) we show the production cross section $\sigma(pp \to H + X)$ for the LHC with the center-of-mass energy of 14 TeV at LO, NLO and NNLO for $M_t = 173.3$ GeV [23], computed with MSTW08 [24] parton distribution function (PDF) set. We collect the numerical results for the LHC with 7 TeV center-of-mass energy and the Tevatron in the Appendix.

The chosen PDFs fix the values of $\alpha_s^{(5)}(M_Z)$ to LO, NLO and NNLO accuracy used as the starting point in order to obtain the strong coupling for the other choices of the renormalization scale. The bands are obtained by varying the renormalization and factorization scales $\mu_r = \mu_f = \mu$ between $M_H/4$ and M_H [25, 26][2] with $\mu = M_H/2$ as central value. For comparison we present the NNLO result computed with ABKM09 PDFs [28] (the dashed line). It is remarkable that the difference in the central values for the different PDFs is comparable to the uncertainty due to the scale variation.

The three-loop term of Eq. (6) contains the logarithm $\ln(\mu^2/M_t^2)$ which can potentially lead to numerically big effects if the scale μ assumes very small or very large values. With the help of C_g and $\mathcal{O}_g$ introduced in Eq. (4) we may introduce separate scales μ_h and μ_s for the hard and the soft parts of the cross section $\sigma = \sigma(\mu_s, \mu_h)$. The dangerous logarithms can then be avoided by choosing $\mu_h \sim M_t$ which is the natural scale for the coefficient function, and varying μ_s around $M_H/2$ as done above. Note that for $\mu_s = \mu_h$ the quantity $B^{(5)}$ drops out of the analysis.

In Fig. 1(b) we plot the ratio $R = \sigma(\mu_s, M_t)/\sigma(\mu_s, \mu_s)$ for $M_H = 120$ GeV. In the numerator the hard scale is kept fixed while in the denominator we use the common approach [4–6]

[1] Here and in the following we suppress the μ-dependence of α_s. If not stated otherwise we have $\alpha_s \equiv \alpha_s(\mu)$. The same is true for the $\overline{\rm DR}$ mass parameters m_t and $m_{\rm susy}$ introduced in Section 3.

[2] For the other opinions concerning the scale variation see Ref. [27].

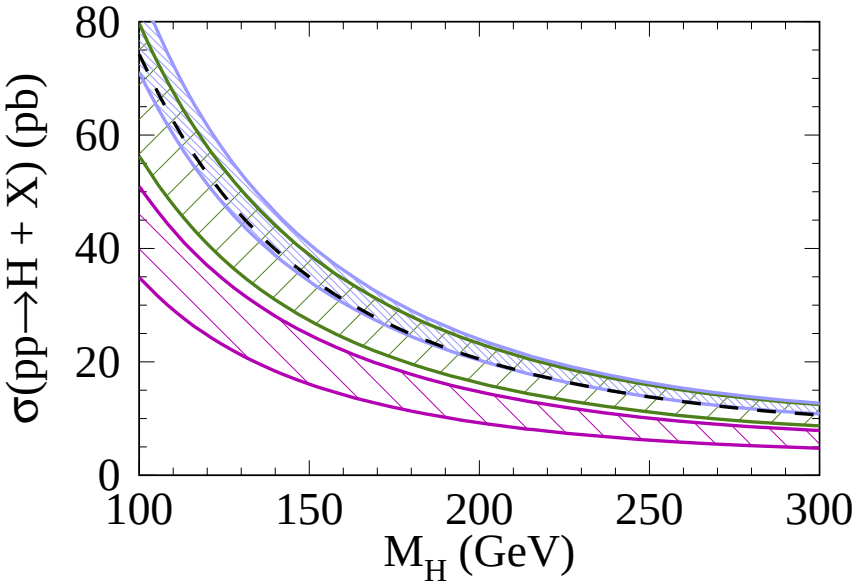

(a)

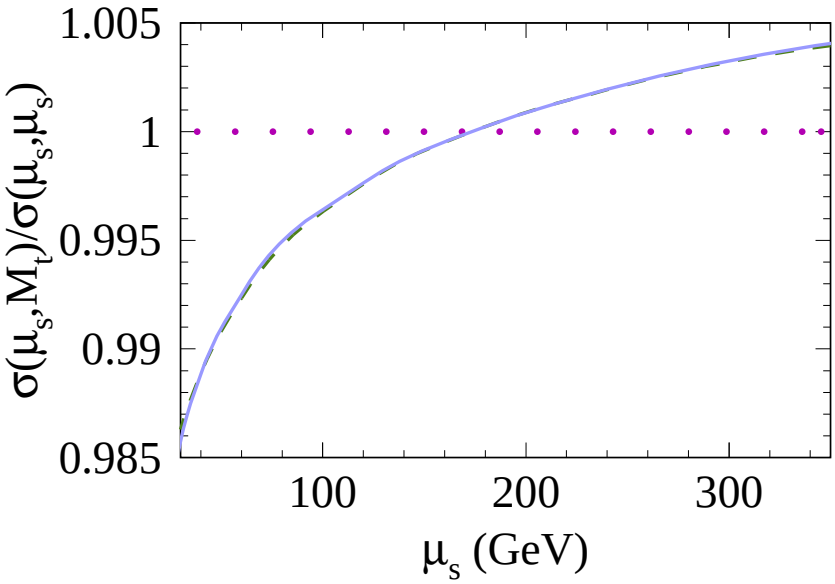

(b)

Figure 1: (a) The SM cross section as a function of M_H. The LO, NLO, and NNLO results are represented by the lower, middle (coarse filling) and the upper bands, respectively. Band width is due to simultaneous variation of renormalization and factorization scales. The dashed line corresponds to the NNLO prediction using ABKM09. (b) Ratio $R = \sigma(\mu_s, M_t)/\sigma(\mu_s, \mu_s)$ for $M_H = 120$ GeV as a function of μ_s. Dotted, dashed (barely visible) and solid lines correspond to LO, NLO and NNLO, respectively.

and identify the scales as in Fig. 1(a). At LO $R = 1$ by construction. The NLO corrections (dashed curve which is hardly visible) are quite small and amount to less than $\pm 2\%$ which is only slightly modified after inclusion of the NNLO results (solid line). From these considerations we conclude that the resummation of $\ln(\mu^2/M_t^2)$ terms has only a small numerical effect. On the other hand, the framework of Eq. (4) is quite useful in the context of supersymmetric corrections discussed below since it allows to fix the hard scale μ_h and vary μ_s.

2.2 $C_1^{\rm SM}$ in DRED

Whereas DRED is the preferable framework for the two- and three-loop calculations in a supersymmetric theory, in the SM the application of DRED introduces several so-called evanescent couplings which can make practical calculations quite tedious. This has been discussed extensively in the literature (see, e.g., Refs. [29–33]). Nevertheless, for our purpose it is useful to evaluate the QCD corrections to the matching coefficient using DRED since there are several new features which also apply to the MSSM.

We implement DRED with the help of the so-called ε scalars. They have mass dimension $(4-d)$ and complement the d-dimensional gluon field so that the gauge fields and the fermions have exactly four degrees of freedom. In a practical calculation the ε scalars induce new Feynman rules (see, e.g., Ref. [34]) which (in non-supersymmetric theories) involve new couplings that have to be renormalized independently from the gauge coupling.

In our matching calculation it is convenient to define $C_1^{\rm SM}$ in such a way that the effective theory is built from the five-flavour QCD fields regularized with DREG. As a consequence, we have to integrate the ε scalar field out together with the top quark in order to guarantee the transition from DRED to DREG in the matching procedure. This means that formally $M_\varepsilon \neq 0$ and even $M_\varepsilon \gg M_H$ since the latter is identical to zero for the matching calculation. In the end, we take the limit $M_\varepsilon \to 0$ in agreement with our renormalization condition (see below).

We evaluate the matching coefficient in the limit $M_t \gg M_\varepsilon \neq 0$ and apply the rules of asymptotic expansion together with a naive expansion in the external momenta in order to project out the Lorentz structure of the Higgs-gluon-gluon vertex (see the following Section for details). Consquently, there are (sub-)diagrams which contain only ε scalars as massive particles. Due to the dimension of the underlying integrals they lead to terms proportional to M_ε^{-2} and M_ε^{-4} in the sum of the bare diagrams. Thus it is necessary to keep positive powers in M_ε in counterterms entering the calculation.

The top quark mass and the strong coupling need to be renormalized at two-loop order. Furthermore, one has to make sure that the external gluon fields of the full and the effective theory Greens functions are identical. There are two operators involved in the renormalization procedure which deserve additional attention: the ε-scalar mass and the coupling of the Higgs boson to ε scalars. The corresponding part of the Lagrange density

is

$$\mathcal{L}_\varepsilon \;=\; -\frac{1}{2}\left(M_\varepsilon^0\right)^2 \varepsilon_\sigma^{0,a}\varepsilon_\sigma^{0,a} - \frac{\phi^0}{v^0}\left(\Lambda_\varepsilon^0\right)^2 \varepsilon_\sigma^{0,a}\varepsilon_\sigma^{0,a} + \dots \,. \tag{7}$$

As mentioned above, we keep $M_\varepsilon \neq 0$ for the matching procedure, however, in the final expression for $C_1^{\rm SM}$ we require that the on-shell M_ε vanishes. This leads to the well-known counterterm (see, e.g., Refs. [20, 35]) which we need to one-loop accuracy. For our purposes we have to keep the terms proportional to M_ε^2 and restore the dependence on all evanescent couplings.

The second term in Eq. (7) is not present at tree-level, however, quantum corrections induce such a structure [8]. We require that the renormalized parameter Λ_ε vanishes since we want to avoid a non-zero coupling between the Higgs boson and the unphysical ε scalars. As a consequence of this condition, we have to introduce a non-zero bare coupling of the Higgs boson to ε scalars. Furthermore, in the counterterm contribution to Λ_ε we only have to keep terms not proportional to Λ_ε. We refrain from listing the explicit results which become quite lengthy due to the evanescent couplings.

It is an important check of our calculation that the negative powers in M_ε cancel after the renomalization of Λ_ε and M_ε.

Our final result for the coefficient function reads:

$$\begin{aligned} C_1^{\overline{\rm DR}} = &-\frac{\alpha_s^{\overline{\rm DR}}}{3\pi}\Bigg\{1 + \frac{\alpha_s^{\overline{\rm DR}}}{\pi}\left(\frac{5}{2} - \frac{1}{6}l_t\right) + \frac{\alpha_s^{\overline{\rm DR}}\alpha_e}{\pi^2}\left(\frac{7}{36} + n_l\frac{1}{12}\right) \\ &+ \left(\frac{\alpha_s^{\overline{\rm DR}}}{\pi}\right)^2\left[\frac{2065}{288} - \frac{5}{48}l_t + \frac{1}{36}l_t^2 - n_l\left(\frac{67}{96} - \frac{1}{3}l_t\right)\right]\Bigg\}, \end{aligned} \tag{8}$$

where $l_{\rm t} = \ln[\mu^2/(m_t(\mu^2))^2]$, $\alpha_s^{\overline{\rm DR}}$ is the strong coupling with six active flavours in the $\overline{\rm DR}$ scheme and α_e is the evanescent coupling originating from the ε scalar-quark vertex. Note that the evanescent coupling stemming from the four-ε-vertex cancels in Eq. (8).

The transition to the five-flavour QCD is achieved with the help of

$$\begin{aligned} \alpha_s^{\overline{\rm DR}} &= \alpha_s^{(5)}\zeta_{\alpha_s}^{-1}\,, \\ \zeta_{\alpha_s}^{-1} &= 1 + \frac{\alpha_s^{(5)}}{\pi}\left[\frac{1}{4} + \frac{1}{6}l_{\rm t} + \epsilon\left(\frac{1}{4}l_\varepsilon + \frac{1}{12}l_{\rm t}^2 + \frac{1}{12}\zeta_2\right)\right] \\ &\quad + \left(\frac{\alpha_s^{(5)}}{\pi}\right)^2\left(\frac{11}{9} + \frac{13}{24}l_{\rm t} + \frac{1}{36}l_{\rm t}^2\right) - \frac{\alpha_s^{(5)}\alpha_e}{\pi^2}\left(\frac{7}{36} + n_l\frac{1}{12}\right)\,. \end{aligned} \tag{9}$$

From Eqs. (8) and (9) we recover $C_1^{\rm SM}$ of Eq. (6)[3] which is a welcome cross check on all individual steps of our calculation, in particular on the counterterms originating from Eq. (7). In the next Section the same framework is applied to the MSSM.

[3]Note that the functional form of Eq. (6) is independent from the quark mass definition.

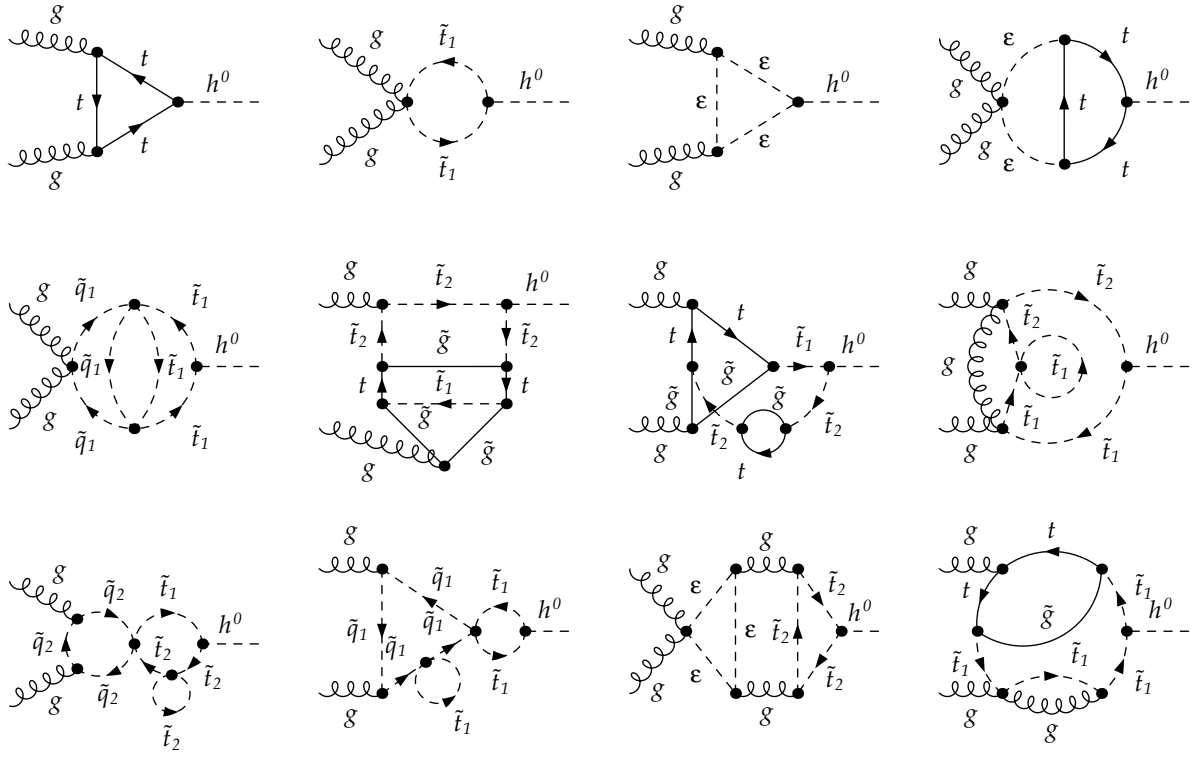

Figure 2: Sample diagrams contributing to C_1 at one, two and three loops. The symbols t, $\tilde{t}_i$, g, $\tilde{g}$, h^0 and ε denote top quarks, top squarks, gluons, gluinos, Higgs bosons and ε scalars, respectively.

3 Coefficient function in the MSSM to three loops

In this Section we describe the evaluation of the coefficient function C_1 of Eq. (1) within the strong sector of the MSSM. Note that the operator $\mathcal{O}_1$ contains the effective interaction of two, three or four gluons with the Higgs boson and we are free to choose any corresponding Greens functions in order to extract C_1. We decided to consider the two-gluon-Higgs boson amplitude since it involves fewer diagrams. We need to keep the two gluon momenta different until the Lorentz structure of O_1 responsible for the two-gluon coupling is projected out.

At one-, two- and three-loop order 10, 671 and 49632 Feynman diagrams have to be considered. Some typical diagrams are shown in Fig. 2. In addition to the particles of supersymmetric QCD we also have the ε scalar. Higgs boson couplings to the light quarks and the corresponding squarks are omitted. Furthermore, we neglect the contribution of the Higgs boson-squark coupling suppressed by M_Z^2/m_t^2 (for the Feynman rules see, e.g., Appendix A of Ref. [7]).

Our calculation is based on a chain of programs designed to minimize the manual input.

First, we generate all the Feynman diagrams with QGRAF [36], then transform the output to FORM [37] notation with the help of q2e and apply asymptotic expansion (see, e.g., Ref. [38]) using exp [39, 40].

Due to the gauge invariance the Higgs-gluon-gluon coupling has the form

$$\mathcal{A}^{\mu\nu,ab} = A\,\delta^{ab}\left(g^{\mu\nu}q_1\cdot q_2 - q_1^\nu q_2^\mu\right), \tag{10}$$

where A is a scalar function depending on $M_H^2 = 2q_1\cdot q_2$, M_t^2, μ^2, and the mass parameters of SUSY QCD. q_1 and q_2 are the outgoing momenta of the gluons with polarization vectors $\varepsilon^\mu(q_1)$ and $\varepsilon^\nu(q_2)$ and colour indices a and b. We begin by convoluting the vertex Feynman diagrams with the projector

$$P^{ab}_{\mu\nu}(q_1,q_2) = \delta^{ab}\frac{q_1\cdot q_2 g_{\mu\nu} - q_{1\mu}q_{2\nu} - q_{1\nu}q_{2\mu}}{8(d-2)(q_1\cdot q_2)^2}, \tag{11}$$

so that only scalar integrals remain. After the Taylor expansion to the linear order in q_1 and q_2 the factor $(q_1\cdot q_2)^2$ in the denominator of Eq. (11) cancels and both momenta can be set to zero. Finally, we evaluate vacuum integrals which (after the asymptotic expansion) only contain a single scale. This is done using the package MATAD [41].

Due to the transverse structure of the Higgs-gluon-gluon amplitude $\mathcal{A}^{\mu\nu,ab}$ an alternative projector to Eq. (11) can be applied to obtain C_1:

$$\tilde{P}^{ab}_{\mu\nu}(q_1,q_2) = \delta^{ab}\frac{q_1\cdot q_2 g_{\mu\nu} - (d-1)q_{1\mu}q_{2\nu} - q_{1\nu}q_{2\mu}}{8(d-2)(q_1\cdot q_2)^2}. \tag{12}$$

We have checked that in both cases we obtain the same result.

One may consider different hierarchies between the mass scales involved in this calculation. As the first choice, we identify all supersymmetric masses with $m_{\rm susy}$ and thus have two expansion parameters, $x_{ts} = m_t/m_{\rm susy}$ and $x_{\varepsilon t} = M_\varepsilon/m_t$. At three-loop order we have computed terms through $\mathcal{O}\left(x_{ts}^6\right)$ and $\mathcal{O}\left(x_{\varepsilon t}^0\right)$. As a cross-check, we performed a similar calculation where the top quark mass and $m_{\rm susy}$ were identified from the very beginning. Comparing the latter result to the former expansion in x_{ts} evaluated at $x_{ts} = 1$ we find agreement to within a few per cent, which serves as a convergence test of our results.

We choose to renormalize all parameters in the $\overline{\rm DR}$ scheme [18]. In particular, we need the counterterms for α_s, the top quark, and the top squark masses to two-loop, and the gluino and other squark mass counterterms to one-loop order. Furthermore, the counterterm for the mixing angle θ_t between the top squarks is also required to the two-loop order. Although θ_t is zero in our approximation, its renormalization in the non-degenerate one- and two-loop expressions leads to non-zero contributions at three-loop level. The corresponding counterterm can either be obtained from the exact one- and two-loop result for C_1 [7], or (as done in this paper) via expansion in the mass difference between the two top squarks. Note that the same effect is also present in the three-loop calculation of the Higgs boson mass within the MSSM, as discussed in Ref. [20, 42]. All

necessary counterterms can be found in the Appendix of Ref. [20] except for the decoupling constant relating the gluon field in the SUSY-QCD to that in the five-flavour QCD, given by

$$\begin{aligned}
\zeta_3^0 =& 1 + \frac{\alpha_s^{(\mathrm{SQCD})}}{\pi}\Bigg\{\frac{1}{\epsilon}\left(\frac{3}{4}+\frac{n_l}{12}\right)+\frac{1}{4}+\frac{7}{12}l_{\mathrm{susy}}+\frac{1}{6}l_t+n_l\frac{1}{12}l_{\mathrm{susy}} \\
&+\epsilon\left[\frac{1}{4}l_\varepsilon+\frac{7}{24}l_{\mathrm{susy}}^2+\frac{1}{12}l_t^2+\frac{3\zeta_2}{8}+n_l\left(\frac{1}{24}l_{\mathrm{susy}}^2+\frac{\zeta_2}{24}\right)\right]\Bigg\} \\
&+\left(\frac{\alpha_s^{(\mathrm{SQCD})}}{\pi}\right)^2\Bigg\{\frac{1}{\epsilon^2}\left(-\frac{69}{64}+n_l\frac{13}{192}+n_l^2\frac{1}{48}\right) \\
&+\frac{1}{\epsilon}\left[\frac{421}{384}-\frac{49}{96}l_{\mathrm{susy}}-\frac{7}{48}l_t+n_l\left(-\frac{25}{384}+\frac{7}{96}l_{\mathrm{susy}}+\frac{1}{24}l_t\right)+n_l^2\frac{1}{48}l_{\mathrm{susy}}\right] \\
&+\frac{1535}{2304}-\frac{7}{32}l_\varepsilon+\frac{53}{192}l_{\mathrm{susy}}+\frac{7}{96}l_{\mathrm{susy}}^2+\frac{29}{96}l_t+\frac{1}{48}l_t^2-\frac{21\zeta_2}{64} \\
&+n_l\left(\frac{97}{2304}+\frac{1}{16}l_\varepsilon-\frac{67}{576}l_{\mathrm{susy}}+\frac{1}{12}l_{\mathrm{susy}}^2+\frac{1}{48}l_t^2+\frac{11\zeta_2}{192}\right) \\
&+n_l^2\left(\frac{1}{96}l_{\mathrm{susy}}^2+\frac{\zeta_2}{96}\right)+x_{ts}^2\left(-\frac{1}{432}-\frac{13}{72}l_{\mathrm{susy}}+\frac{5}{72}l_t\right)\Bigg\}+\mathcal{O}\left(x_{ts}^4\right)\,, \qquad (13)
\end{aligned}$$

where $l_{\mathrm{susy}} = \ln[\mu^2/(m_{\mathrm{susy}}(\mu^2))^2]$ and $\alpha_s^{(\mathrm{SQCD})}$ denotes the $\overline{\mathrm{DR}}$ coupling where all particles of the theory contribute to the running. In Eq. (13) $n_l = 5$ counts the number of massless quarks and at the same time the number of squark flavours different from top squarks. Similarly to the SM case in Section 2.2, we keep $M_\varepsilon \neq 0$ in the intermediate steps in order to match to the effective theory of Eq. (1). Thus, M_ε and the coupling Λ_ε (cf. Eq. (7)) have to be renormalized with the help of the counterterms

$$\begin{aligned}
\left(M_\varepsilon^0\right)^2 &= M_\varepsilon^2+\frac{\alpha_s^{(\mathrm{SQCD})}}{\pi}\Bigg\{m_t^2\left(\frac{1}{2\epsilon}+\frac{1}{2}+\frac{1}{2}l_{\mathrm{t}}\right)+M_\varepsilon^2\Bigg[\frac{8-n_l}{4\epsilon}+\frac{9}{2}+3l_\varepsilon-\frac{3}{4}l_{\mathrm{susy}}-\frac{1}{4}l_{\mathrm{t}} \\
&\quad+\left(-\frac{1}{2}-\frac{1}{4}l_\varepsilon\right)n_l\Bigg]+m_{\mathrm{susy}}^2\left[1+l_{\mathrm{susy}}+\frac{2-nl}{2\epsilon}+\left(-\frac{1}{2}-\frac{1}{2}l_{\mathrm{susy}}\right)n_l\right]\Bigg\}\,, \qquad (14)
\end{aligned}$$

with $l_\varepsilon = \ln[\mu^2/M_\varepsilon^2]$, and

$$
\begin{aligned}
\left(\Lambda_\varepsilon^0\right)^2 - \Lambda_\varepsilon^2 &= \delta\Lambda_\varepsilon^2 \\
&= -2m_t^2 \frac{c_\alpha}{s_\beta} \Bigg\{ \frac{\alpha_s^{(\mathrm{SQCD})}}{\pi} \left[\frac{1}{2} l_{\mathrm{susy}} - \frac{1}{2} l_t + \epsilon \left(\frac{1}{4} l_{\mathrm{susy}}^2 - \frac{1}{4} l_t^2 \right) \right] \\
&\quad + \left(\frac{\alpha_s^{(\mathrm{SQCD})}}{\pi} \right)^2 \left[\frac{1}{\epsilon} \left(-l_{\mathrm{susy}} + l_t + n_l \left(\frac{1}{8} l_{\mathrm{susy}} - \frac{1}{8} l_t \right) \right) \right. \\
&\quad + \frac{1}{3} + \frac{23}{12} l_{\mathrm{susy}} - \frac{1}{8} l_{\mathrm{susy}}^2 - \frac{23}{12} l_t - \frac{1}{12} l_{\mathrm{susy}} l_t + \frac{5}{24} l_t^2 + n_l \left(\frac{1}{16} l_{\mathrm{susy}}^2 - \frac{1}{16} l_t^2 \right) \\
&\quad \left. + x_{ts} x_{\mu t} \left(t_\alpha + \frac{1}{t_\beta} \right) \left(\frac{11}{12} + \frac{1}{6} l_{\mathrm{susy}} + \frac{1}{6} l_t \right) + x_{ts}^2 \left(-\frac{359}{216} + \frac{19}{72} l_{\mathrm{susy}} - \frac{67}{72} l_t \right) \right] \Bigg\} \\
&\quad + \mathcal{O}(x_{ts}^4) + \mathcal{O}(x_{ts}^3 x_{\mu t}) \,, \qquad (15)
\end{aligned}
$$

where $c_\alpha = \cos\alpha$, $s_\beta = \sin\beta$, $t_\alpha = \tan\alpha$, $t_\beta = \tan\beta$ and $x_{\mu t} = \mu_{\mathrm{susy}}/m_t$. Here α is the mixing angle between the weak and the mass eigenstates of the neutral scalar Higgs bosons, $\tan\beta$ is the ratio of the vacuum expectation values of the two Higgs doublets, and μ_{susy} is the Higgs-Higgsino bilinear coupling from the super potential. Note that the counterterm for Λ_ε and the three-loop vertex diagrams have been evaluated assuming the same hierarchy of the top quark and the top squark masses. Let us mention that the counterterm in Eq. (15) is finite at one-loop order and only contains a single pole at two loops whereas the corresponding expression in QCD has a single and a double pole, respectively.

In the first step we obtain C_1 in terms of $\alpha_s^{(\mathrm{SQCD})}$. It is, however, more convenient to express the final result in terms of the five-flavour coupling in the $\overline{\mathrm{MS}}$ scheme $\alpha_s^{(5)} = \alpha_s^{(5),\overline{\mathrm{MS}}}$. The relation establishing this transition is as follows:

$$
\alpha_s^{(5)} = \zeta_{\alpha_s} \alpha_s^{(\mathrm{SQCD})} \,. \qquad (16)
$$

Two-loop corrections to the decoupling constant ζ_{α_s} within supersymmetric QCD have been computed in Refs. [43–45]. Since ζ_{α_s} in Eq. (16) combines the decoupling of the heavy particles and the transition from $\overline{\mathrm{DR}}$ to $\overline{\mathrm{MS}}$, we present the explicit result in the limit of equal supersymmetric masses:

$$
\begin{aligned}
\zeta_{\alpha_s} &= 1 + \frac{\alpha_s^{(\mathrm{SQCD})}}{\pi} \left(-\frac{1}{4} - \frac{7}{12} l_{\mathrm{susy}} - \frac{1}{6} l_{\mathrm{t}} - n_l \frac{1}{12} l_{\mathrm{susy}} \right) + \left(\frac{\alpha_s^{(\mathrm{SQCD})}}{\pi} \right)^2 \left[\frac{77}{288} \right. \\
&\quad - \frac{5}{8} l_{\mathrm{susy}} + \frac{49}{144} l_{\mathrm{susy}}^2 - \frac{3}{8} l_{\mathrm{t}} + \frac{7}{36} l_{\mathrm{susy}} l_{\mathrm{t}} + \frac{1}{36} l_{\mathrm{t}}^2 + n_l \left(\frac{23}{144} - \frac{1}{72} l_{\mathrm{susy}} + \frac{7}{72} l_{\mathrm{susy}}^2 \right. \\
&\quad \left. \left. + \frac{1}{36} l_{\mathrm{susy}} l_{\mathrm{t}} \right) + n_l^2 \frac{1}{144} l_{\mathrm{susy}}^2 + \left(\frac{1}{432} + \frac{13}{72} l_{\mathrm{susy}} - \frac{5}{72} l_{\mathrm{t}} \right) x_{ts}^2 \right] + \mathcal{O}(x_{ts}^4) \,. \qquad (17)
\end{aligned}
$$

All occurring mass parameters and the top squark mixing angle have been renormalized in the $\overline{\rm DR}$ scheme.

Finally, we present the coefficient function C_1 expressed in terms of $\overline{\rm DR}$ masses and the mixing angle, expanded in $\alpha_s^{(5)}$:

$$
\begin{aligned}
C_1^{\overline{\rm DR}} &= -\frac{\alpha_s^{(5)}}{3\pi}\frac{c_\alpha}{s_\beta}\Bigg\{1+\frac{x_{ts}^2}{2}+\frac{\alpha_s^{(5)}}{\pi}\Bigg[\frac{11}{4}-\frac{1}{3}\left(t_\alpha+\frac{1}{t_\beta}\right)\frac{\mu_{\rm susy}}{m_{\rm susy}}+\Bigg(\frac{23}{12}+\frac{5}{12}l_{\rm susy} \\
&\quad -\frac{5}{12}l_{\rm t}\Bigg)x_{ts}^2\Bigg]+\left(\frac{\alpha_s^{(5)}}{\pi}\right)^2\Bigg[\frac{2777}{288}+\frac{19}{16}l_{\rm t}+\left(-\frac{67}{96}+\frac{1}{3}l_{\rm t}\right)n_l \\
&\quad +\left(-\frac{85}{54}-\frac{85}{108}l_{\rm susy}-\frac{1}{18}l_{\rm t}+\left(-\frac{1}{18}+\frac{1}{12}l_{\rm susy}\right)n_l\right)\left(t_\alpha+\frac{1}{t_\beta}\right)\frac{\mu_{\rm susy}}{m_{\rm susy}} \\
&\quad +\Bigg(\frac{30779857}{648000}-\frac{2429}{10800}l_{\rm susy}-\frac{475}{288}l_{\rm susy}^2-\frac{24007}{10800}l_{\rm t}+\frac{26}{45}l_{\rm susy}l_{\rm t}-\frac{377}{1440}l_{\rm t}^2 \\
&\quad -\frac{15971}{576}\zeta_3+\Bigg(-\frac{3910697}{216000}+\frac{63}{4}\zeta_3+\frac{4907}{4800}l_{\rm susy}+\frac{131}{576}l_{\rm susy}^2+\frac{313}{14400}l_{\rm t} \\
&\quad -\frac{101}{1440}l_{\rm susy}l_{\rm t}+\frac{3}{320}l_{\rm t}^2\Bigg)n_l\Bigg)x_{ts}^2\Bigg]\Bigg\}+\mathcal{O}\left(x_{ts}^4\right)+\mathcal{O}\left(\frac{\mu_{\rm susy}}{m_{\rm susy}}x_{ts}^3\right)\,. \qquad (18)
\end{aligned}
$$

The analytic expression including $\mathcal{O}(x_{ts}^6)$ and $\mathcal{O}(\frac{\mu_{\rm susy}}{m_{\rm susy}}x_{ts}^5)$ is available on request from the authors. It is noteworthy that in the limit $m_{\rm susy}\to\infty$ we recover exactly the SM result of Eq. (6).

4 Higgs boson production at NNLO

In this Section we discuss the numerical effect of the corrections presented above. The effective-theory parts in the MSSM and the SM are identical, and thus we can borrow the framework of Ref. [2]. In addition, we incorporate the factor $B^{(5)}$ (in the $\overline{\rm MS}$ scheme) as discussed in the Introduction.

On the full-theory side we consider the renormalization group invariant combination $C_g = C_1/B^{(5)}$ where both C_1 and $B^{(5)}$ are parameterized with the five-flavour strong coupling in the $\overline{\rm MS}$ scheme. For the numerical evaluation of $C_1^{\overline{\rm DR}}$ we fix the (hard) renormalization scale at the on-shell top quark mass value, i.e. $\mu_h = M_t$, which means that the $\overline{\rm DR}$ mass parameters in Eq. (18) have to be interpreted as $m_{\rm susy}(M_t)$ and $m_t(M_t)$. Any variation of μ_h leads to a non-degenerate supersymmetric spectrum and thus renders Eq. (18) not applicable. As shown in Section 2 (Fig. 1(b)), the variation of μ_h only leads to a very small effect and thus we keep it fixed.

Following the common practice, we write the hadronic cross section for the individual

channels as

$$\sigma_{hk}(s) \;=\; \sigma_0 C_g^2 \Sigma_{hk}(s)\,, \tag{19}$$

where $hk \in \{gg, qg, q\bar{q}, qq, qq'\}$ (q and q' denote different light quark flavours) and σ_0 contains the exact dependence on the heavy masses at the LO. In the SM this is only the top quark mass, while in the MSSM also the top squark masses $m_{\tilde{t}_1} = m_{\tilde{t}_2} = m_{\rm susy}$ must be taken into account[4]:

$$\sigma_0 \;=\; \left| \frac{c_\alpha}{s_\beta} \left\{ \frac{3}{2}\tau_t \left[1 + (1-\tau_t)\right] f(\tau_t) - \frac{m_t^2}{2m_{\rm susy}^2} 3\tau_s \left[1 - \tau_s f(\tau_s)\right] \right\} + \mathcal{O}\left(\frac{M_W^2}{m_t^2}\right) \right|^2 . \tag{20}$$

where $\tau_t = 4m_t^2/M_H^2$, $\tau_s = 4m_{\rm susy}^2/M_H^2$ and

$$f(t) = \begin{cases} \arcsin^2(1/\sqrt{t}), & t >= 1\,, \\ -\frac{1}{4}\left(\ln\frac{1+\sqrt{1-t}}{1-\sqrt{1-t}} - i\pi\right)^2, & t < 0\,. \end{cases} \tag{21}$$

The quantity $\Sigma_{hk}(s)$ in Eq. (19), expanded in $\alpha_s^{(5)}(\mu_s)$, contains the convolutions of the PDFs with the n-loop ($n = 0, 1, 2$) effective-theory partonic cross sections. In the SM, such effective theory approach provides an excellent approximation at NNLO [1–3]. Once the LO cross section which depends on $\alpha_s^{(5)}(\mu_s)$ is factored out, we are left with a product of the residual hard coefficient depending on $\alpha_s^{(5)}(\mu_h)$ and the remaining part of $\Sigma_{hk}(s)$ which is parameterized in terms of $\alpha_s^{(5)}(\mu_s)$. We expand these factors and consistently discard higher orders in the strong coupling, decomposing the hadronic cross section into the LO, NLO and NNLO pieces. Introducing

$$\begin{aligned} C_g &= 1 + \frac{\alpha_s^{(5)}(\mu_h)}{\pi} c_g^{(1)} + \left(\frac{\alpha_s^{(5)}(\mu_h)}{\pi}\right)^2 c_g^{(2)} + \dots\,, \\ \Sigma &= 1 + \frac{\alpha_s^{(5)}(\mu_s)}{\pi} \Sigma^{(1)} + \left(\frac{\alpha_s^{(5)}(\mu_s)}{\pi}\right)^2 \Sigma^{(2)} + \dots\,, \end{aligned} \tag{22}$$

we write the production cross section as

$$\begin{aligned} \sigma^{\rm NNLO} \;=\; \sigma^{\rm LO} \Bigg\{ & \Sigma^{(0)} + \frac{\alpha_s^{(5)}(\mu_s)}{\pi}\Sigma^{(1)} + \frac{\alpha_s^{(5)}(\mu_h)}{\pi} 2c_g^{(1)}\Sigma^{(0)} + \left(\frac{\alpha_s^{(5)}(\mu_s)}{\pi}\right)^2 \Sigma^{(2)} \\ & + \frac{\alpha_s^{(5)}(\mu_s)}{\pi}\frac{\alpha_s^{(5)}(\mu_h)}{\pi} 2c_g^{(1)}\Sigma^{(1)} + \left(\frac{\alpha_s^{(5)}(\mu_h)}{\pi}\right)^2 \left[(c_g^{(1)})^2 + 2c_g^{(2)}\right]\Sigma^{(0)} + \dots \Bigg\}, \end{aligned} \tag{23}$$

where superscripts on c_g or Σ denote the loop order of the corresponding quantity.

[4]The terms of order M_W^2/m_t^2 are not displayed but are accounted for in the numerical evaluation.

As input for the numerical evaluation we use the on-shell top quark mass $M_t = 173.3$ GeV [23]. By default we use LO, NLO and NNLO PDFs by MSTW2008 collaboration [24]. For comparison, we compute the same results using ABKM09 [28] PDFs. The choice of the PDFs determines the values of $\alpha_s^{(5)}(M_Z)$ at the considered order. Using the appropriate $\overline{\rm MS}$ beta function, we then derive $\alpha_s^{(5)}(\mu_s)$ and $\alpha_s^{(5)}(\mu_h)$.

In Fig. 3(a) we show the production cross section for the supersymmetric mass $m_{\rm susy}(M_t) = 200$ GeV and $m_t(M_t) = 163.7$ GeV. The latter value has been obtained with the help of the on-shell-$\overline{\rm DR}$ conversion formula of Ref. [46]. The values of the supersymmetric parameters were chosen as $\alpha = -0.1$ and $\tan\beta = 10$, which gives $\cos\alpha/\sin\beta \approx 1$ so that the direct comparison with the SM becomes possible.

As in Fig. 1(a), the bands represent the soft scale variation between $M_H/4$ and M_H, and the dashed line corresponds to the central value of the NNLO result computed with ABKM09 PDFs. One observes a pattern very similar to the SM: there is a relatively big gap between the LO and NLO, although the LO error band is quite sizeable. The latter is significantly reduced at NNLO. Furthermore, we observe an overlap of the NLO and NNLO uncertainty bands. As already discussed above there is a big difference between the ABKM09 and MSTW08 PDFs which is of the order of the scale uncertainty. Analogous results for the LHC with 7 TeV center-of-mass energy and the Tevatron can be found in the Appendix.

In Fig. 3(b) we show the MSSM production cross section as a function of $m_{\rm susy}$. For the values of $m_{\rm susy}$ below ≈ 500 GeV one observes a clear deviation of the MSSM prediction from the SM values (shown as dashed lines). For the larger values of $m_{\rm susy}$ the squark and gluino contributions become negligible.

In order to compare to the SM it is convenient to consider the so-called K-factor where the higher order corrections are normalized to the Born cross section with the soft scale fixed at $\mu_s^2 = (M_H/2)^2$, i.e.

$$K^{\rm HO} \;=\; \frac{\sigma^{\rm HO}(\mu_s)}{\sigma^{\rm LO}(\mu_s = M_H/2)}\,. \tag{24}$$

In Fig. 4(a) and (b) we plot the K-factor of the SM and MSSM corrections as a function of M_H (for $m_{\rm susy} = 200$ GeV) and $m_{\rm susy}$ (with $M_H = 120$ GeV), respectively. The uncertainty bands in (a) result from the variation of μ_s. The SM results are shown as dashed lines. One observes only a minor difference between the MSSM and the SM predictions for the K factor which becomes completely negligible for $m_{\rm susy} \gtrsim 250$ GeV.

5 Conclusions

In this letter we have computed supersymmetric NNLO SUSY-QCD corrections to the matching coefficient determining the Higgs-gluon coupling in the effective theory. Regularization was done in `DRED` with the help of the so-called ε scalars which made the

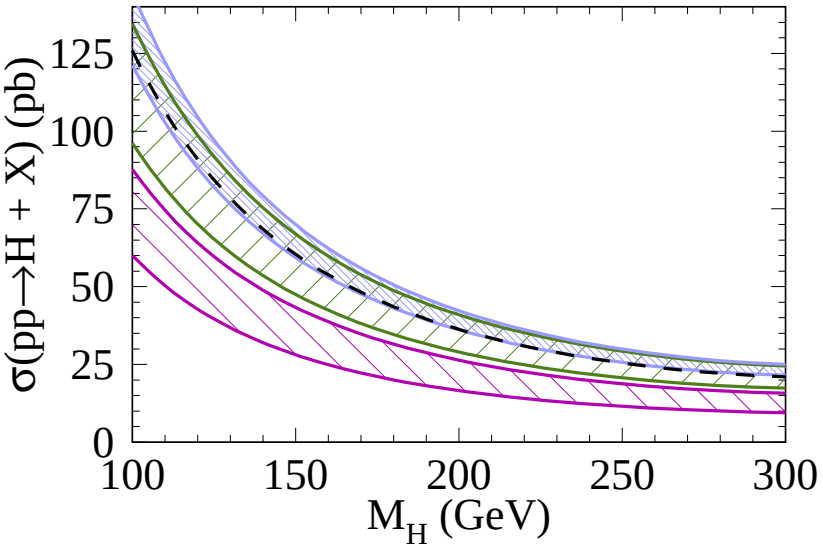

(a)

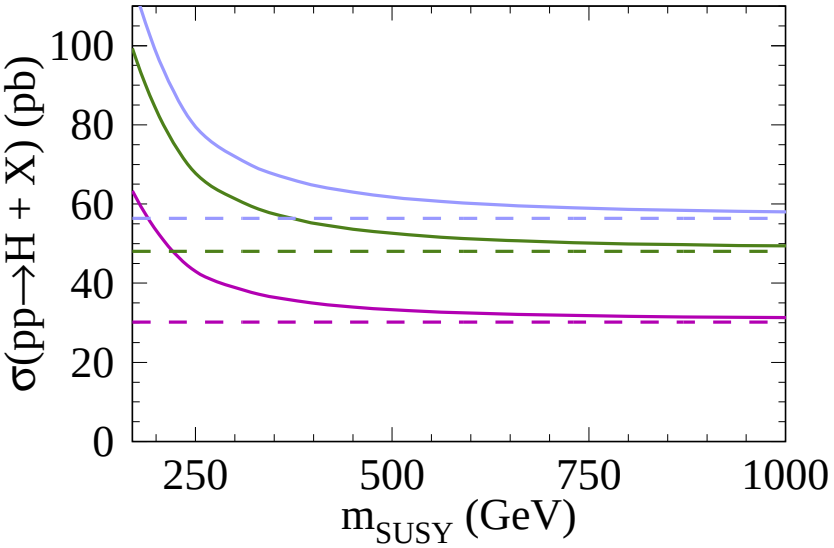

(b)

Figure 3: (a) LO (lower band), NLO (middle band, coarse fill-style) and NNLO (upper band) Higgs production cross section in the MSSM for the degenerate mass spectrum $m_{\rm susy}(M_t) = 200$ GeV as a function of M_H. The dashed line corresponds to the ABKM09 PDFs and the bands to the uncertainty due to scale variation. (b) LO (lower lines), NLO (middle lines) and NNLO (upper lines) Higgs production cross section in the MSSM as a function of $m_{\rm susy}$ for $M_H = 120$ GeV and $\mu_s = M_H/2$. The dashed lines correspond to the SM results.

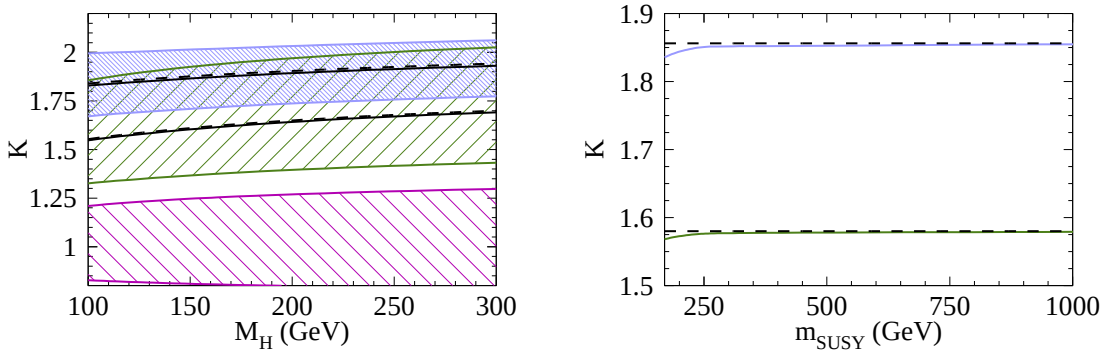

(a) (b)

Figure 4: K-factor in the SM and MSSM as a function of M_H (a) and $m_{\rm susy}$ (b). In (a) the lower, middle and upper bands correspond to the LO, NLO and NNLO corrections.

matching to the five-flavour QCD very delicate. In particular, we had to renormalize the mass of the ε scalar and its coupling to the Higgs boson at one- and two-loop orders, respectively.

As far as higher order corrections are concerned, in the MSSM we observe the same pattern as in the SM: large NLO corrections which further increase at NNLO. Compared to the SM, we see an increase of the cross section which can be as large as 50%. However, the MSSM K factors are very close to the SM counterparts. This confirms the estimate of Ref. [14] based on the complete NLO corrections to the matching coefficient and the NNLO calculation in the effective theory.

Our calculation has been performed in the limit of degenerate supersymmetric masses. In order to explore all interesting regions of the supersymmetric parameter space it would be necessary to relax this restriction. Since a three-loop calculation with many different mass scales is currently not feasible it is more promising to employ a strategy based on asymptotic expansions which has been applied successfully to predict the lightest MSSM Higgs boson mass in Ref. [20].

Appendix: numerical results for LHC7 and Tevatron

In this Appendix we fix $m_{\rm susy}(M_t) = 200$ GeV and present the numerical results for the LO, NLO and NNLO cross section and the K factor for the LHC with center-of-mass energy of 7 TeV (LHC7) (Fig. 5) and the Tevatron (Fig. 6).

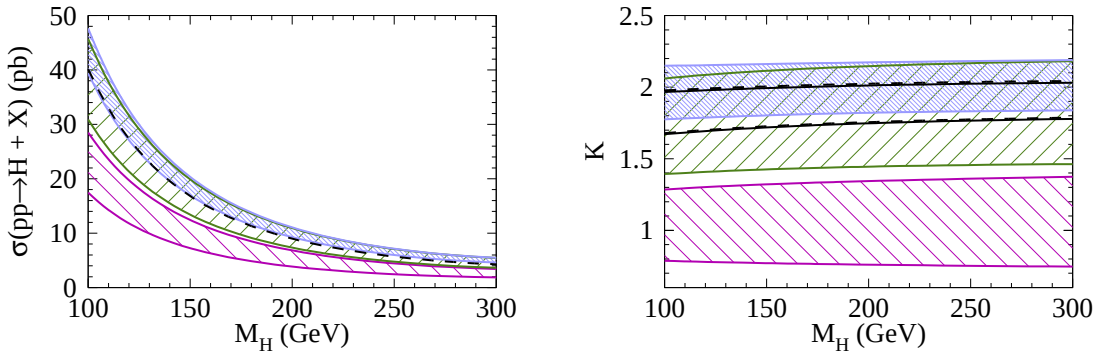

Figure 5: Results for the LHC7: (a) LO, NLO and NNLO Higgs production cross section in the MSSM and (b) K factor. Lines and fill-styles are as in Figs. 3 and 4.

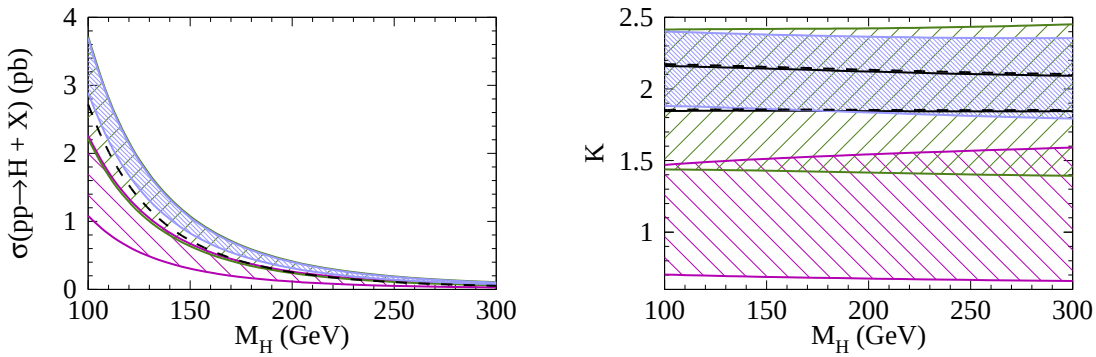

(a) (b)

Figure 6: Results for the Tevatron: (a) LO, NLO and NNLO Higgs production cross section in the MSSM and (b) K factor. Lines and fill-styles are as in Figs. 3 and 4.

Acknowledgements

This work was supported by the DFG through the SFB/TR 9 "Computational Particle Physics" and the Graduiertenkolleg "Hochenergiephysik und Teilchenastrophysik".

References

[1] R. V. Harlander and K. J. Ozeren, JHEP **0911** (2009) 088 [arXiv:0909.3420 [hep-ph]].

[2] A. Pak, M. Rogal and M. Steinhauser, JHEP **1002** (2010) 025 [arXiv:0911.4662 [hep-ph]].

[3] R. V. Harlander, H. Mantler, S. Marzani and K. J. Ozeren, arXiv:0912.2104 [hep-ph].

[4] R. V. Harlander and W. B. Kilgore, Phys. Rev. Lett. **88** (2002) 201801, arXiv:hep-ph/0201206.

[5] C. Anastasiou and K. Melnikov, Nucl. Phys. B **646** (2002) 220, arXiv:hep-ph/0207004.

[6] V. Ravindran, J. Smith and W. L. van Neerven, Nucl. Phys. B **665** (2003) 325, arXiv:hep-ph/0302135.

[7] R. V. Harlander and M. Steinhauser, JHEP **0409** (2004) 066 [arXiv:hep-ph/0409010].

[8] C. Anastasiou, S. Beerli and A. Daleo, Phys. Rev. Lett. **100** (2008) 241806 [arXiv:0803.3065 [hep-ph]].

[9] R. V. Harlander and M. Steinhauser, Phys. Lett. B **574** (2003) 258 [arXiv:hep-ph/0307346].

[10] G. Degrassi and P. Slavich, Nucl. Phys. B **805** (2008) 267 [arXiv:0806.1495 [hep-ph]].

[11] M. Muhlleitner, H. Rzehak and M. Spira, arXiv:1001.3214 [hep-ph].

[12] R. Bonciani, G. Degrassi and A. Vicini, JHEP **0711** (2007) 095 [arXiv:0709.4227 [hep-ph]].

[13] M. Muhlleitner and M. Spira, Nucl. Phys. B **790** (2008) 1 [arXiv:hep-ph/0612254].

[14] R. Harlander and M. Steinhauser, Phys. Rev. D **68** (2003) 111701 [arXiv:hep-ph/0308210].

[15] V. P. Spiridonov, INR Report No. P-0378 (1984).

[16] K. G. Chetyrkin, B. A. Kniehl and M. Steinhauser, Nucl. Phys. B **510** (1998) 61, arXiv:hep-ph/9708255.

[17] K. G. Chetyrkin, B. A. Kniehl and M. Steinhauser, Nucl. Phys. B **490** (1997) 19 [arXiv:hep-ph/9701277].

[18] W. Siegel, Phys. Lett. B **84** (1979) 193.

[19] R. V. Harlander, L. Mihaila and M. Steinhauser, Eur. Phys. J. C **63** (2009) 383 [arXiv:0905.4807 [hep-ph]].

[20] P. Kant, R. V. Harlander, L. Mihaila and M. Steinhauser, JHEP **1008** (2010) 104 [arXiv:1005.5709 [hep-ph]].

[21] M. Steinhauser, Phys. Rept. **364** (2002) 247, arXiv:hep-ph/0201075.

[22] M. Kramer, E. Laenen and M. Spira, Nucl. Phys. B **511** (1998) 523 [arXiv:hep-ph/9611272].

[23] Tevatron Electroweak Working Group [CDF and D0 Collaboration], arXiv:1007.3178 [hep-ex].

[24] A. D. Martin, W. J. Stirling, R. S. Thorne and G. Watt, Eur. Phys. J. C **63** (2009) 189 [arXiv:0901.0002 [hep-ph]].

[25] C. Anastasiou, R. Boughezal and F. Petriello, JHEP **0904** (2009) 003 [arXiv:0811.3458 [hep-ph]].

[26] M. Grazzini, PoS **RADCOR2009** (2010) 047 [arXiv:1001.3766 [hep-ph]].

[27] J. Baglio and A. Djouadi, JHEP **1010** (2010) 064 [arXiv:1003.4266 [hep-ph]].

[28] S. Alekhin, J. Blumlein, S. Klein and S. Moch, Phys. Rev. D **81** (2010) 014032 [arXiv:0908.2766 [hep-ph]].

[29] I. Jack, D. R. T. Jones and K. L. Roberts, Z. Phys. C **62** (1994) 161 [arXiv:hep-ph/9310301].

[30] I. Jack, D. R. T. Jones and K. L. Roberts, Z. Phys. C **63** (1994) 151 [arXiv:hep-ph/9401349].

[31] R. Harlander, P. Kant, L. Mihaila and M. Steinhauser, JHEP **0609** (2006) 053 [arXiv:hep-ph/0607240].

[32] R. V. Harlander, D. R. T. Jones, P. Kant, L. Mihaila and M. Steinhauser, JHEP **0612** (2006) 024 [arXiv:hep-ph/0610206].

[33] I. Jack, D. R. T. Jones, P. Kant and L. Mihaila, JHEP **0709** (2007) 058 [arXiv:0707.3055 [hep-th]].

[34] P. Kant, "Higgs-Masse im MSSM und dimensionale Reduktion in hohen Ordnungen der Störungstheorie," (PhD thesis, University of Karlsruhe, 2009).

[35] P. Marquard, L. Mihaila, J. H. Piclum and M. Steinhauser, Nucl. Phys. B **773** (2007) 1, arXiv:hep-ph/0702185.

[36] P. Nogueira, J. Comput. Phys. **105** (1993) 279.

[37] J. A. M. Vermaseren, arXiv:math-ph/0010025.

[38] V. A. Smirnov, "Applied asymptotic expansions in momenta and masses," Springer Tracts Mod. Phys. **177** (2002) 1.

[39] R. Harlander, T. Seidensticker and M. Steinhauser, Phys. Lett. B **426** (1998) 125, arXiv:hep-ph/9712228.

[40] T. Seidensticker, arXiv:hep-ph/9905298.

[41] M. Steinhauser, Comput. Phys. Commun. **134** (2001) 335, arXiv:hep-ph/0009029.

[42] R. V. Harlander, P. Kant, L. Mihaila and M. Steinhauser, Phys. Rev. Lett. **100** (2008) 191602 [Phys. Rev. Lett. **101** (2008) 039901] [arXiv:0803.0672 [hep-ph]].

[43] R. Harlander, L. Mihaila and M. Steinhauser, Phys. Rev. D **72** (2005) 095009 [arXiv:hep-ph/0509048].

[44] A. Bauer, L. Mihaila and J. Salomon, JHEP **0902** (2009) 037 [arXiv:0810.5101 [hep-ph]].

[45] A. V. Bednyakov, Int. J. Mod. Phys. A **22** (2007) 5245 [arXiv:0707.0650 [hep-ph]].

[46] S. P. Martin, Phys. Rev. D **72**, 096008 (2005) [arXiv:hep-ph/0509115].